Atmos. Chem. Phys. Discuss., doi:10.5194/acp-2016-1065, 2016
Manuscript under review for journal Atmos. Chem. Phys.
Published: 19 December 2016

Atmospheric Chemistry and Physics
Discussions
Open Access
EGU

Title

Enhanced Stratospheric Water Vapor over the Summertime Continental United States and the Role of Overshooting Convection

Robert L. Herman[1], Eric A. Ray[2], Karen H. Rosenlof[2], Kristopher M. Bedka[3], Michael J. Schwartz[1], William G. Read[1], Robert F. Troy[1], Keith Chin[1], Lance E. Christensen[1], Dejian Fu[1], Robert A. Stachnik[1], T. Paul Bui[4], Jonathan M. Dean-Day[5]

[1]Jet Propulsion Laboratory, California Institute of Technology, Pasadena, California, USA.
[2]National Oceanic and Atmospheric Administration (NOAA) Earth System Research Laboratory (ESRL) Chemical Sciences Division, Boulder, Colorado, USA.
[3]NASA Langley Research Center, Hampton, Virginia, USA.
[4]NASA Ames Research Center, Moffett Field, California, USA.
[5]Bay Area Environmental Research Institute, Sonoma, California, USA.
Correspondence to: R. L. Herman (Robert.L.Herman@jpl.nasa.gov)

Atmos. Chem. Phys. Discuss., doi:10.5194/acp-2016-1065, 2016
Manuscript under review for journal Atmos. Chem. Phys.
Published: 19 December 2016

Atmospheric Chemistry and Physics
Open Access
Discussions

Abstract

The NASA ER-2 aircraft sampled the UTLS region over North America during the NASA Studies of Emissions and Atmospheric Composition, Clouds and Climate Coupling by Regional Surveys (SEAC^{4}RS) field mission. This study reports three case studies of convectively-influenced air parcels with enhanced water vapor in the overworld stratosphere over the summertime continental United States. Water vapor mixing ratios greater than 10 ppmv, more than twice the stratospheric background levels, were measured by the JPL Laser Hygrometer (JLH Mark2) at pressure levels between 80 and 160 hPa. Through satellite observations and analysis, we make the connection between these *in situ* water measurements and overshooting cloud tops. The overshooting tops (OT) are identified from a SEAC^{4}RS OT detection product based on satellite infrared window channel brightness temperature gradients. Back trajectory analysis ties enhanced water to OT one to seven days prior to the intercept by the aircraft. The trajectory paths are dominated by the North American Monsoon (NAM) anticyclonic circulation. This connection suggests that ice is convectively transported to the overworld stratosphere in OT events and subsequently sublimated; such events may irreversibly enhance stratospheric water vapor in the summer over Mexico and the United States. Regional context is provided by water observations from the Aura Microwave Limb Sounder (MLS).

Keywords

Convection, overshoot, atmospheric water, stratosphere-troposphere exchange

Atmos. Chem. Phys. Discuss., doi:10.5194/acp-2016-1065, 2016
Manuscript under review for journal Atmos. Chem. Phys.
Published: 19 December 2016

1. Introduction

Water plays a predominant role in the radiative balance of the Earth's atmosphere, both in the gas phase as the Earth's primary greenhouse gas and in condensed phases in cloud and aerosol. Despite its low abundance, upper tropospheric and lower stratospheric (UTLS) water vapor is critically important in controlling outgoing long-wave radiation, and quantifying UTLS water vapor and its controlling processes is critical for climate characterization and prediction. Climate models are sensitive to changes in stratospheric water (Shindell, 2001) and clouds (Boucher et al., 2013). Increases in UTLS water are associated with warming at the surface on the decadal scale (Solomon et al., 2010). As the dominant source of hydroxyl radicals, UTLS water also plays an important role in control of UTLS ozone (Shindell, 2001; Kirk-Davidoff et al., 1999).

The stratospheric "overworld", the altitude region with potential temperature θ greater than 380 K (Holton et al. 1995), is extremely dry, with typical mixing ratios of 3—6 parts per million by volume (ppmv). The importance of low temperatures at the tropical tropopause acting as a "cold trap" to prevent tropospheric water from entering the stratosphere has been recognized since Brewer (1949). Tropospheric air slowly ascends through the tropical tropopause layer (TTL) as part of the hemispheric-scale Brewer-Dobson circulation. In the TTL, air passes through extremely cold regions where water vapor condenses in situ to form cirrus ice, and then the cirrus slowly falls due to sedimentation (e.g., Jensen et al., 2013). Additional condensation and sedimentation are thought to be associated with convection and large-scale waves (e.g., Voemel et al., 2002). The amount of water that enters the stratosphere is largely a function of the coldest temperature a parcel trajectory encounters. This typically occurs in the tropics, and the coldest temperature is typically near the tropical tropopause. The saturation mixing ratio at the cold point tropopause thereby sets the entry value of water vapor.

In contrast to water entry into the stratospheric overworld, water transport from the troposphere to the lowermost stratosphere (θ < 380 K) commonly occurs through several different pathways. Poleward of the subtropical jet, water can be transported into the lowermost stratosphere through isentropic troposphere-stratosphere exchange (Holton et al., 1995) or through convective overshoot of the local tropopause (Dessler et al., 2007; Hanisco et al., 2007). How important sublimation of ice from convective overshoot is for hydrating the stratosphere is a topic of ongoing debate (e.g., Randel et al., 2015; Wang, 2003). Case studies have reported extreme events where elevated water is transported to the overworld stratosphere, but the amount of ice that is irreversibly injected into the stratosphere is poorly known. Airborne measurements have demonstrated that convective injection occurs both in the tropics (Webster and Heymsfield, 2003; Corti et al., 2008; Sayres et al., 2010; Sargent et al., 2014) and at mid-latitudes (Hanisco et al., 2007; Anderson et al., 2012). Ice injected directly into the overworld stratosphere bypasses the TTL cold trap (Ravishankara, 2012). Paraphrasing Bedka et al. (2010), a convective overshooting top (OT) is a protrusion above a cumulonimbus anvil due to strong updrafts above the equilibrium level. Early observations of OT include photographs of OT in the stratosphere from a U-2 aircraft (Roach 1967). Recent observations of elevated water mixing ratios in the summer overworld stratosphere by aircraft (Anderson et al., 2012) and the Aura Microwave Limb Sounder (MLS) (Schwartz et al., 2013) suggest that ice injection into the overworld stratosphere by OT, while rare, occurs in three predominant regions during the summer season. These three regions are the

Atmos. Chem. Phys. Discuss., doi:10.5194/acp-2016-1065, 2016
Manuscript under review for journal Atmos. Chem. Phys.
Published: 19 December 2016

Atmospheric Chemistry and Physics
Discussions

Asian Monsoon region, the South American continent, and – the focus of this study - the North American Monsoon (NAM) region (Schwartz et al., 2013).

The NASA ER-2 aircraft sampled the summer UTLS in the NAM region during the NASA Studies of Emissions and Atmospheric Composition, Clouds and Climate Coupling by Regional Surveys (SEAC^{4}RS) field mission (Toon et al., 2016). One of the primary goals of this multi-aircraft mission was to address the question: do deep convective cloud systems locally inject water vapor and other chemicals into the overworld stratosphere over the continental United States (CONUS)? It is difficult for space- and ground-based techniques to detect enhanced water vapor injected into the stratosphere by OT. Satellite measurements are limited in their spatial resolution to detect fine-scale variations in water vapor, while ground-based measurements are confined to sampling at fixed locations. In contrast, airborne *in situ* UTLS measurements of water have an advantage because the aircraft can be routed to a specific location, altitude, date and time. Modelers can predict whether air parcels are likely to have convective influence, and aircraft flight paths are planned to intercept those air parcels. The purpose of this paper is to report three new case studies of enhanced water vapor in the overworld stratosphere during the NASA SEAC^{4}RS field mission, and to connect these observations to deep convective OT over the North American continent.

2. Observations

2.1 Aircraft

The airborne *in situ* water vapor measurements reported here are from the Jet Propulsion Laboratory Laser Hygrometer Mark2 (JLH Mark2), a tunable laser spectrometer with an open-path cell external to the aircraft fuselage (May, 1998). Water vapor is reported at 1 Hz (10% accuracy), although the time response of the open-path cell is much faster than this because the instrument is sampling the free-stream airflow. This instrument has a redesigned optomechanical structure for greater optical stability, and was first flown in this configuration on the NASA ER-2 high-altitude aircraft during the SEAC^{4}RS field mission. Pressure and temperature, provided by the Meteorological Measurement System (MMS) (Scott et al., 1990), are used in the data processing to calculate water vapor mixing ratios from spectra, as described in May (1998).

During SEAC^{4}RS, nine aircraft flights targeted air parcels with recent convective influence (see Table 3 of Toon et al., 2016). Instruments on the NASA ER-2 aircraft indicated that the aircraft intercepted convectively-influenced air. Both the JLH Mark2 instrument and other water vapor sensors on the ER-2 observed enhanced stratospheric water vapor above background levels. The largest enhancements were observed on three flights that are described in detail in Sect. 4.

2.2 Aura MLS

Aura MLS measures daily global atmospheric profiles of species including water vapor. While the aircraft samples *in situ* water in a thin trajectory through the atmosphere, Aura MLS provides a larger scale context. Expanding on the analysis of Schwartz et al. (2013), Aura MLS observations of stratospheric water vapor are presented here for the SEAC[4]RS time period of summer 2013. Aura MLS H_2O has 0.4 ppmv precision at 100 hPa for individual profile measurements, with spatial representativeness of 200 km along line-of-sight (Schwartz et al., 2013). Results shown here use MLS version 3.3 data, but are not significantly different when recast with the newer version 4.2. MLS observations over CONUS are at ~14:10 local time (ascending orbit) and~1:20 local time (descending orbit), with successive swaths separated by ~1650 km. Vertical resolution of the water vapor product is ~3 km in the UTLS (Livesey et al., 2013). Aura MLS shows a seasonal maximum in water vapor over CONUS in July and August. Figure 1 adds the 2013 SEAC[4]RS time period to the long-term Aura MLS 100-hPa time series from Schwartz et al. (2013). This figure shows the summertime higher mean H_2O as well as extreme outliers mostly during July and August (shaded gray). The decadal histogram of Figure 2 shows that, in 2013, the CONUS lower stratosphere was relatively dry compared to the previous multi-year MLS record. Nevertheless, enhanced UTLS water vapor was observed by MLS in 2013 as rare but detectable events. Figure 3 shows that, out of all MLS 100-hPa water vapor retrievals over the two-month period July to August 2013, water greater than 8 ppmv was measured only nine times over North America and four times near Central America.

3. Analysis

Here we briefly describe the analytical technique used to determine whether back trajectories from the aircraft location intersect OT as identified by a satellite OT data product.

3.1 Detection of overshooting tops

In order to link the stratospheric UTLS water vapor encountered by the aircraft to the storm systems that sourced them, it is necessary to have a comprehensive continental scale catalog of deep convection. Geostationary Operational Environmental Satellite (GOES) infrared imagery is used to assemble a catalog of OTs throughout the U.S. and offshore waters. This catalog was acquired from the NASA LaRC Airborne Science Data From Atmospheric Composition data archive (http://www-air.larc.nasa.gov/cgi-bin/ArcView/seac4rs). Because OTs are correlated with storm intensity, the OT product was primarily developed to benefit the aviation community for more accurate turbulence prediction, as well as the general public for earlier severe storm warnings. However, the product is also ideally suited for identifying storm systems that can moisten the stratosphere.

Infrared brightness temperatures are used to detect cloud top temperature anomalies within thunderstorm anvils. OT candidates are colder than the mean surrounding anvil, with the temperature difference indicative of both the strength of the convective updraft and the depth of penetration. Additional validation of OTs requires comparison with the Global Forecast System (GFS) Numerical Weather Prediction (NWP) model tropopause temperature. The maximum OT cloud height was derived based on knowledge of the 1) OT-anvil temperature difference, 2) the anvil cloud height based on a match of the anvil mean temperature near to the OT and the GFS NWP temperature profile, and 3) a temperature lapse rate within the UTLS region based on a GOES-derived OT-anvil temperature difference and NASA CloudSat OT-anvil height difference for a sample of direct CloudSat OT overpasses (Griffin et al., 2016). For SEAC[4]RS, every available GOES-East and GOES-West scan (typically 15 min resolution) was processed

Atmos. Chem. Phys. Discuss., doi:10.5194/acp-2016-1065, 2016
Manuscript under review for journal Atmos. Chem. Phys.
Published: 19 December 2016

for the full duration of the mission, even for the non-flight days, yielding a detailed and comprehensive picture of the location, timing, and depth of penetration of convective storms over the entire CONUS. The output files include the OT coordinates, time, overshooting intensity in degrees K – which is related to the temperature difference between the OT and the anvil – and an estimate of maximum cloud height for OT pixels in meters.

3.2 Back trajectory modeling

Back trajectories were run from each flight profile where enhanced water vapor was measured to determine whether the sampled air was convectively influenced. The trajectories were run with the FLEXPART model (Stohl et al., 2005) using NCEP Climate Forecast System version 2 (CFSv2) meteorology (Saha et al., 2014). Trajectories were initialized every second along the flight track profiles and run backward for seven days. A sampled air parcel was determined to be convectively influenced if the back trajectory from that parcel intercepted an OT region. The tolerances for a trajectory to be considered to have intercepted an OT cloud were +/-0.25 degrees latitude and longitude, +/-3 hours, +/-0.5 km in altitude.

4. Case Studies

In this section, we highlight three NASA ER-2 flights where elevated stratospheric water was observed by JLH Mark2. These dates are 8, 16 and 27 August 2013. Similar results are seen from other hygrometers on the NASA ER-2 aircraft. For each of these ER-2 flights, seven-day back trajectory analyses are initialized at locations and times of enhanced water vapor along the ER-2 flight track. These analyses are combined with overshooting cloud top data from the SEAC^{4}RS OT data product. The cases are described below.

4.1 First case: 8 August 2013

This flight was the transit flight from Palmdale, California to Ellington Field, Houston, Texas. In addition to sending the NASA ER-2 aircraft to the destination base, the science goal of this flight was to profile the North American Monsoon region with five profiles plus the aircraft ascent and final descent. This flight shows a dramatic transition from west to east of background stratospheric water to enhanced water (Figures 4a, b, c). In the lowermost stratosphere (θ<380 K), water can be highly variable, but at 90 hPa it is generally unusual to observe water vapor greater than 6 ppmv. As shown in Figure 4a, the color-coded stratospheric water vapor mixing ratios are 4.0 to 4.4 ppmv at 90 hPa (17 km) over the west coast of CONUS (black and blue points). There is a gradient in water vapor from west to east, with 7 ppmv water at 90 hPa over west Texas (green points), and 11 ppmv at 90 hPa over eastern Texas (red points). Simultaneous Aura MLS retrievals also demonstrate a west-to-east water vapor gradient on this day (solid lines in Figures 4a, b, c).

To gain insight into the sources of the enhanced stratospheric water, we run back trajectory calculations initialized at locations of enhanced water. In Figures 5, 6, and 7 that follow, for clarity only some example trajectories (a subset of our analysis) are shown. These are displayed as thin blue traces in panels (b) and (c). The initial water vapor mixing ratios of the example trajectories are shown as red squares in panels (a). The intersections of the example trajectories with coincident OT are shown as red squares in panels (b) and (c). All overshooting convective tops within the looser tolerances prescribed (see Sect. 3.2) for *all* back trajectories are shown by green symbols in panels (b) and (c).

Analysis of the 8 August 2013 case is shown in Figure 5. Back trajectories from the flight track follow the anticyclonic NAM circulation over Western Mexico, Great Plains and Mississippi Valley (Figure 5b). Every one of the example back trajectories intersects OT, as shown by red symbols in Figure 5b. For this flight, coincidences with overshooting convection are dominated by overshooting clouds over the Mississippi Valley and Great Plains. All overshooting convection within the tolerances prescribed (see Sect. 3.2) for the back trajectories are shown by the green symbols in Figure 5b and 5c. Figure 5c demonstrates the range of altitudes reached by the coincident overshooting convection and how many convective overshooting cells were coincident. The high resolution of the convective overshooting data meant that there could be multiple coincident convective overshooting cells for a single location on a back trajectory. It is significant that some of the green overshooting cells are higher altitude than the red coincident points, suggesting that overshooting air parcels descended slightly before mixing with the surrounding air. Figure 5d indicates the source of enhanced water was dominated by overshooting clouds two to five days earlier than intercept by the aircraft.

4.2 Second case: 16 August 2013

The NASA ER-2 flight of 16 August 2013 was designed to survey the North American Monsoon in a triangular flight path from Houston, Texas, to the Imperial Valley in Southern California, to Southeastern Colorado and back to Texas. The NASA ER-2 aircraft performed six dives, encountering enhanced stratospheric water at 16 to 17 km altitude (Figure 6a). As shown in Figure 6b, back trajectories intersect overshooting tops over the Central U.S. (Texas, Oklahoma, Arkansas) and also over the Sierra Madre Occidental mountain range on the west coast of Mexico. This case is an example of the classic North American Monsoon circulation with a moisture source over the Sierra Madre Occidental. Anticyclonic transport carried the moisture north from Mexico, and counter-clockwise around the high pressure (Figure 6b). The altitude range of the convective overshoot is typically 16 to 17 km altitude, as shown in Figure 6c. The time between OT and intercept by the aircraft ranges from two to seven days (Figure 6d).

4.3 Third case: 27 August 2013

The 27 August 2013 flight performed six dives to sample the North American Monsoon. Stratospheric water was enhanced to 15 to 20 ppmv in altitudes ranging from 16.0 to 17.5 km (Figure 7a). The ER-2 aircraft intercepted highly enhanced stratospheric water from a MCC over the Upper Midwest, which had overshooting tops over Northern Minnesota and Northern Wisconsin (Toon et al., 2016), as shown in Figure 7b. Figure 7c shows an abundance of OT above 17 km (green). Generally speaking, the OT appear at higher altitudes in the northern CONUS/southern Canada than in the Central CONUS. Figure 7d shows that the air masses were sampled *in situ* by the ER-2 aircraft over Illinois and Indiana one to two days after the intense storm. As is a common theme for all these experiment days, a portion of the back-trajectories also trace back to overshooting tops over the Sierra Madre Occidental one week prior.

5. Conclusions

In this paper we have examined *in situ* measurements of stratospheric water by JLH Mark2 on the ER-2 aircraft during the SEAC^{4}RS field mission. With JLH Mark2 data, enhanced H_2O above background mixing ratios was frequently encountered in the lowermost stratosphere between 160 and 80 hPa. Example air parcel back-trajectories were initialized at the locations and time of enhanced water. All of the back-trajectories connect these air parcels to convective OT one to seven days prior to aircraft intercept. The trajectory modeling indicates that the identified OT are associated with larger storm systems over the Central U.S., and also deep convection over the Sierra Madre Occidental.

The concentrations of enhanced water and the connection to OT suggests a mechanism for moistening the CONUS lower stratosphere: ice is irreversibly injected into the overworld stratosphere by the most intense convective tops. The temperatures of the CONUS lower stratosphere are sufficiently warm to sublimate the ice, leaving behind water vapor elevated up to 15 ppmv above background mixing ratios. The summertime CONUS has a high frequency of thunderstorms with sufficient energy to transport ice to the upper troposphere (Koshak et al., 2015, and references therein). On rare occasion, these storms have sufficient energy to propel water through the tropopause and into the stratosphere. Ice sublimation is supported by the enriched delta-D isotopic signature in water vapor observed by the ACE satellite over summertime North America (Randel et al., 2010). Cross-tropopause transport is a consequence of turbulent mixing at cloud top, possibly enhanced by the existence of breaking gravity waves often occurring near overshooting cloud tops. (Wang, 2003).

This study addresses a primary goal of the SEAC^{4}RS field mission (Toon et al., 2016), answering affirmatively the science question: “Do deep convective cloud systems locally inject water vapor and other chemicals into the overworld stratosphere over the CONUS?” This water is almost certainly injected in the ice phase and subsequently sublimated in the relatively warm stratosphere over CONUS, leading to irreversible hydration. From this study, we conclude that the depth of injection was typically 16 to 17.5 km altitude for these particular summertime events.

Satellite retrievals of water vapor from Aura MLS provide a larger-scale context. Elevated water vapor at the 100-hPa level was observed infrequently by Aura MLS. Limb measurements from Aura MLS come from a long (~200 km) path through the atmosphere so locally water vapor may be enhanced even more. At the 100-hPa level in the lower stratosphere, the year 2013 was slightly drier than the average of 2004-2013 summers but, nevertheless, there was sufficient enhanced water to be clearly observed in the Aura MLS retrievals.

In situ measurements probe on a small-scale air parcels that can be connected to OT that inject ice and, to a lesser extent, trace gases to the stratosphere (e.g., Ray et al., 2004; Hanisco et al., 2007; Jost et al, 2004). In contrast,

Atmos. Chem. Phys. Discuss., doi:10.5194/acp-2016-1065, 2016
Manuscript under review for journal Atmos. Chem. Phys.
Published: 19 December 2016

modeling studies tend to focus on large-scale processes. Dessler et al. (2002) and Corti et al. (2008) concluded that OT are a significant source of water vapor in the mid-latitude lower stratosphere. In contrast, Randel et al. (2015) used Aura MLS observations to conclude that circulation plays a larger role than OT in controlling mid-latitude stratospheric water vapor in the monsoon region. Our study shows clear evidence of observable perturbations to stratospheric water vapor on ER-2 aircraft flights that targeted convectively-influenced air during SEAC^{4}RS. The fraction of Aura MLS observations in the same time period with H_2O greater than 8 ppmv is very small, on the order of 1%. This reinforces the conclusion of Randel et al. (2015) that OT play a minor role in the mid-latitude stratospheric water budget. In future work, we plan more detailed back trajectory analysis of air parcels over summertime North America to better understand the transport of ice and water in the lower stratosphere.

Atmos. Chem. Phys. Discuss., doi:10.5194/acp-2016-1065, 2016
Manuscript under review for journal Atmos. Chem. Phys.
Published: 19 December 2016

Code Availability

n/a

Data Availability

Data discussed in this manuscript are publically available. The NASA aircraft data are available through the following digital object identifier (DOI): SEAC4RS DOI 10.5067/Aircraft/SEAC4RS/Aerosol-TraceGas-Cloud.

Appendices: none

Supplement link: none

Team List:

Robert L. Herman[1], Eric A. Ray[2], Karen H. Rosenlof[2], Kristopher M. Bedka[3], Michael J. Schwartz[1], William G. Read[1], Robert F. Troy[1], Keith Chin[1], Lance E. Christensen[1], Dejian Fu[1], Robert A. Stachnik[1], T. Paul Bui[4], Jonathan M. Dean-Day[5]

[1]Jet Propulsion Laboratory, California Institute of Technology, Pasadena, California, USA.
[2]National Oceanic and Atmospheric Administration (NOAA) Earth System Research Laboratory (ESRL) Chemical Sciences Division, Boulder, Colorado, USA.
[3]NASA Langley Research Center, Hampton, Virginia, USA.
[4]NASA Ames Research Center, Moffett Field, California, USA.
[5]Bay Area Environmental Research Institute, Sonoma, California, USA.

Author Contribution

Robert Herman prepared the manuscript with contributions from all coauthors and was responsible for all aspects of the JLH Mark2 as principal investigator. Eric Ray and Karen Rosenlof provided trajectory calculations and interpretation. Kristopher Bedka provided an overshooting top data product and interpretation. Robert Troy, Robert Stachnik and Keith Chin operated the JLH Mark2 instrument in the field and downloaded data. Robert Stachnik, Dejian Fu, Lance Christensen and Keith Chin also developed software components for the JLH Mark2 instrument. Michael Schwartz and William Read provided Aura MLS data and statistical analysis. T. Paul Bui and Jonathan Dean-Day measured pressure and temperature with the MMS instrument and provided data.

Competing interests:

The authors declare that they have no conflict of interest.

Disclaimer

Acknowledgements

Atmos. Chem. Phys. Discuss., doi:10.5194/acp-2016-1065, 2016
Manuscript under review for journal Atmos. Chem. Phys.
Published: 19 December 2016

Atmospheric Chemistry and Physics Discussions

We thank Jose Landeros and Dave Natzic for providing technical support in the laboratory and field, and the aircraft crew and flight planners for making these measurements possible. The JLH Mark2 team is supported by the NASA Upper Atmosphere Research Program and Radiation Sciences Program. Part of this research was performed at JPL, California Institute of Technology, under a contract with NASA.

References

Anderson, J. G., Wilmouth, D. M., Smith, J. B., and Sayres, D. S.: UV Dosage Levels in Summer: Increased Risk of Ozone Loss from Convectively Injected Water Vapor, Science, 337(6096), 835-839, 2012.

Bedka, K. M., J. Brunner, R. Dworak, W. Feltz, J. Otkin, and T. Greenwald: Objective satellite-based overshooting top detection using infrared window channel brightness temperature gradients. *J. Appl. Meteor. And Climatol.*, **49**, 181-202, 2010.

Boucher, O., Randall, D., Artaxo, P., Bretherton, C., Feingold, G., Forster, P., Kerminen, V.-M., Kondo, Y., Liao, H., Lohmann, U., Rasch, P., Satheesh, S. K., Sherwood, S., Stevens B., and Zhang, X. Y.: Clouds and Aerosols. In: Climate Change 2013: The Physical Science Basis. Contribution of Working Group I to the Fifth Assessment Report of the Intergovernmental Panel on Climate Change (Stocker, T. F., Qin, D., Plattner, G.-K., Tignor, M., Allen, S. K., Boschung, J., Nauels, A., Xia, Y., Bex, V., and Midgley, P. M. (eds.)), Cambridge University Press, Cambridge, United Kingdom and New York, NY, USA, 2013.

Brewer, A. W.: Evidence for a world circulation provided by the measurements of helium and water vapor distribution in the stratosphere, *Q. J. Roy. Met. Soc.,* 75, 351-63, 1949.

Corti, T., Luo, B. P., De Reus, M., Brunner, D., Cairo, F., Mahoney, M. J., Martucci, G., Matthey, R., Mitev, V., Dos Sntos, F. H., Schiller, C., Shur, G., Sitnikov, N. M., Spelten, N., Voessing, H. J., Borrmann, S., and Peter, T.: Unprecedented evidence for deep convection hydrating the tropical stratosphere, *Geophys. Res. Lett., 35,* L10810, doi:10.1029/2008GL033641, 2008.

Dessler, A. E., Hanisco, T. F, and Fueglistaler, S.: Effects of convective ice lofting on H_2O and HDO in the tropical tropopause layer, *J. Geophys. Res., 112*, doi:10.1029/2007JD008609, 2007.

Griffin, S. M., Velden, C. S., and Bedka, K. M.: A method for calculating the height of overshooting convective cloud tops using satellite-based IR imager and CloudSat cloud profiling radar observations, J. Appl. Met. and Clim., 55, 479-491, DOI: http://dx.doi.org/10.1175/JAMC-D-15-0170.1, 2016.

Hanisco, T. F., Moyer, E. J., Weinstock, E. M., St. Clair, J. M., Sayres, D. S., Smith, J. B., Lockwood, R., Anderson, J. G., Dessler, A. E., Keutsch, F. N., Spackman, J. R., Read, W. G., and Bui, T. P.: Observations of deep convective influence on stratospheric water vapor and its isotopic composition, *Geophys. Res. Lett., 34,* L04814, doi:10.1029/2006GL027899, 2007.

Holton, J.R., P.H. Haynes, A.R. Douglass, R.B. Rood, and L. Pfister: Stratosphere–troposphere exchange. Rev. Geophys., 33(4), 403–439, 1995.

Jensen, E. J., Diskin, G., Lawson, R. P., Lance, S., Bui, T. P., Hlavka, D., McGill, M., Pfister, L., Toon, O. B., and Gao, R., Ice nucleation and dehydration in the Tropical Tropopause Layer, Proc. Nat. Acad. Sci., 110(6), 2041–2046, 2013.

Jensen, E. J., Smith, J. B., Pfister, L., Pittman, J. V., Weinstock, E. M., Sayres, D. S., Herman, R. L., Troy, R. F., Rosenlof, K., Thompson, T. L., Fridlind, A. M., Hudson, P. K., Cziczo, D. J., Heymsfield, A. J., Schmitt, C. and Wilson, J. C.: Ice Supersaturations Exceeding 100% at the Cold Tropical Tropopause: Implications for Cirrus Formation and Dehydration, Atmos. Chem. Phys., 5, 851-62, 2005.

Atmos. Chem. Phys. Discuss., doi:10.5194/acp-2016-1065, 2016
Manuscript under review for journal Atmos. Chem. Phys.
Published: 19 December 2016

Jost, H. J., et al.: In-situ observations of mid-latitude forest fire plumes deep in the stratosphere, Geophys. Res. Lett., 31, L11101, doi:10.1020/2003GL019253, 2004.

Kirk-Davidoff, D. B., Hintsa, E. J., Anderson, J. G., and Keith, D. W.: The effect of climate change on ozone depletion through changes in stratospheric water vapour, *Nature, 402*, 399-401, doi:10.1038/46521, 1999.

Koshak, W. J., Cummins, K. L., Buechler, D. E., Vant-Hull B., Blakeslee, R. J., Williams, E. R., and H. S. Peterson: Variability of CONUS Lightning in 2003-12 and Associated Impacts, *J. Appl. Meteor. Climat., 54*, 15-41,doi:10.1175/JAMC-D-14-0072.1, 2015.

Livesey, N. J., et al.: Earth Observing System (EOS) Aura Microwave Limb Sounder (MLS) Version 3.3 and 3.4 Level 2 data quality and description document, Tech. Rep. JPL D-33509, Jet Propulsion Laboratory, 2013. Available online at http://mls.jpl.nasa.gov, 2013.

Liu, C., Zipser, E. J., Cecil, D. J., Nesbitt, S. W., Sherwood, S.: *J. Appl. Meteorol. Climatol. 47*, 2712: 2008.

May, R. D.: Open-path, near-infrared tunable diode laser spectrometer for atmospheric measurements of H_2O, J. Geophys. Res., 103(D15), 19161-19172, doi:10.1029/98jd01678, 1998.

Moyer, E., Irion, F., Yung, Y., and Gunson, M.: ATMOS stratospheric deuterated water and implications for troposphere-stratosphere transport, *Geophys. Res. Lett., 23*(17), 2385-88, 1996.

Randel, W. J., K. Zhang, and R. Fu: What controls stratospheric water vapor in the NH summer monsoon regions?, *J. Geophys. Res.*, 120, 7988–8001, doi:10.1002/2015JD023622, 2015.

Ravishankara, A. R.: Water Vapor in the Lower Stratosphere, Science, 337, 809–810, doi: 10.1126/science.1227004, 2012.

Ray, E. A., Rosenlof, K. H., Richard, E. C., Hudson, P. K., Cziczo, D. J., Loewenstein, M., Jost, H.-J., Lopez, J., Ridley, B., Weinheimer, A., Montzka, D., Knapp, D., Wofsy, S. C., Daube, B. C., Gerbig, C., Xueref, I., and Herman, R. L.: Evidence of the effect of summertime midlatitude convection on the subtropical lower stratosphere from CRYSTAL-FACE tracer measurements, J. Geophys. Res., 109(D18), D18304, doi: 10.1029/2004JD004655, 2004.

Read, W. G., et al.: Aura Microwave Limb Sounder upper tropospheric and lower stratospheric H_2O and relative humidity with respect to ice validation, J. Geophys. Res. Atmospheres, 112(D24), D24S35, doi:10.1029/2007jd008752, 2007.

Roach, W. T.: On the nature of the summit areas of severe storms in Oklahoma, *Q. J. R. Meteorol. Soc., 93*, 318–336, 1967.

Rodgers, C. D.: Inverse Methods for Atmospheric Sounding: Theory and Practice, World Science, London, 2000.

Rodgers, C. D., and Connor, B. J.: Intercomparison of Remote Sounding Instruments, J. Geophys. Res., 108, 4116, doi: 10.1029/2002JD002299, 2003.

Saha, S. et al.: The NCEP Climate Forecast System Version 2, J. Climate, 27, 2185–2208, doi:10.1175/JCLI-D-12-00823.1, 2014.

Sargent, M. R., Smith, J. B., Sayres, D. S., and Anderson, J. G.: The roles of deep convection and extratropical mixing in the Tropical Tropopause Layer: An in situ measurement perspective, *J. Geophys. Res., 119*(21), 12355-71, DOI:10.1002/2014JD022157, 2014.

Atmos. Chem. Phys. Discuss., doi:10.5194/acp-2016-1065, 2016
Manuscript under review for journal Atmos. Chem. Phys.
Published: 19 December 2016

Atmospheric Chemistry and Physics Discussions
Open Access

Sayres, D. S., Pfister, L., Hanisco, T. F., Moyer, E. J., Smith, J. B., St. Clair, J. M., O'Brien, A. S., Witinski, M. F., Legg, M., and Anderson, J. G.: Influence of convection on the water isotopic composition of the tropical tropopause layer and tropical stratosphere, *J. Geophys. Res., 115,* D00J20, doi:10.1029/2009JD013100, 2010.

Schwartz, M. J., Read, W. G., Santee, M. L., Livesey, N. J., Froidevaux, L., Lambert, A., and Manney, G. L.: Convectively injected water vapor in the North American summer lowermost stratosphere, Geophys. Res. Lett., 40, 2316-2321, doi:10.1002/grl.50421, 2013.

Scott, S. G., Bui, T. P., Chan, K. R., and Bowen, S. W.: The meteorological measurement system on the NASA ER-2 aircraft, J. Atmos. Ocean. Tech., 7, 525-40, 1990.

Shindell, D. T.: Climate and ozone response to increased stratospheric water vapor, *Geophys. Res. Lett., 28,* 1551-4, 2001.

Smith, J. B., Sargent, M., Wilmouth, D. and Anderson, J. G.: Quantifying the Direct Convective Transport of Tropospheric Air to the Overworld Statosphere, Abstract A51O-0288, presented at 2015, Fall Meeting, AGU, San Francisco, CA, 14-18 December, 2015.

Solomon, S., Rosenlof, K. H., Portmann, R. W., Daniel, J. S., Davis, S. M., Sanford, T. J., and Plattner, G.-K.: Contributions of Stratospheric Water Vapor to Decadal Changes in the Rate of Global Warming, Science, 327(5970), 1219-1223, doi:10.1126/science.1182488, 2010.

Stohl, A., C. Forster, A. Frank, P. Seibert, and G. Wotawa: Technical note: The Lagrangian particle dispersion model FLEXPART version 6.2, Atmos. Chem. Phys., 5, 2461-2474, doi: 10.5194/acp-5-2461-2005-supplement, 2005.

Toon, O. B., H. Maring, J. Dibb, R. Ferrare, D. J. Jacob, E. J. Jensen, Z. J. Luo, G. G. Mace, L. L. Pan, L. Pfister, K. H. Rosenlof, J. Redemann, J. S. Reid, H. B. Singh, A. M. Thompson, R. Yokelson, P. Minnis, G. Chen, K. W. Jucks, and A. Pszenny: Planning, implementation and scientific goals of the Studies of Emissions and Atmospheric Composition, Clouds and Climate Coupling by Regional Surveys ($SEAC^4RS$) field mission, *J. Geophys. Res., 121*, 4967-5009, doi:10.1002/2015JD024297, 2016.

Voemel, H., et al.: Balloon-borne observations of water vapor and ozone in the tropical upper troposphere and lower stratosphere, *J. Geophys. Res.*, 107(D14), pages ACL 8-1-ACL 8-16, DOI:10.1029/2001JD000707, 2002. Available online at http://onlinelibrary.wiley.com/doi/10.1029/2001JD000707/full#jgrd8979-fig-0017, 2002.

Wang, P. K., Moisture plumes above thunderstorm anvils and their contributions to cross-tropopause transport of water vapor in midlatitudes, *J. Geophys. Res., 108*(D6), 4194, doi:10.1029/2002JD002581, 2003.

Webster, C. R., and Heymsfield, A. J.: Water Isotope Ratios D/H, $^{18}O/^{16}O$, $^{17}O/^{16}O$ in and out of Clouds Map Dehydration Pathways, *Science*, 302, 1742, DOI: 10.1126/science.1089496, 2003.

Atmos. Chem. Phys. Discuss., doi:10.5194/acp-2016-1065, 2016
Manuscript under review for journal Atmos. Chem. Phys.
Published: 19 December 2016

Atmospheric Chemistry and Physics
Open Access
EGU
Discussions

TABLES

Table 1 Summary of airborne enhanced water vapor case studies during SEAC[4]RS*.

Date	Maximum H_2O (ppmv)	Altitude range (km) of enhanced H_2O	Source region (from back-trajectories)
8 August 2013	11.2	16.5 to 17.7	Great Plains, Mex.
16 August 2013	12.2	16.3 to 17.2	AK, OK, TX, Mex.
27 August 2013	20.5	15.9 to 17.5	MN, WI, Mexico

* SEAC[4]RS = Studies of Emissions and Atmospheric Composition, Clouds and Climate Coupling by Regional Surveys

FIGURE CAPTIONS

Figure 1. Time series of Aura MLS v3.3 100-hPa H_2O over North America. Each monthly histogram is normalized to unity over mixing ratio. Dashed black vertical lines mark year boundaries, and gray-shaded areas denote July-August. Data are from the eastern CONUS through northern Mexico (see Figure 2 insert), a study box empirically chosen to enclose the highest outliers associated with the North American Monsoon in the 10+ year MLS 100-hPa water vapor climatology (after Schwartz et al., 2013).

Figure 2. Distribution of Aura MLS July-August 100-hPa H_2O over North America (blue shaded box in insert) for July-August 2013 (blue line) and July-August ten-year mean for 2004 to 2013 (red line).

Figure 3. Aura MLS 100-hPa H_2O (color scale), with superimposed MERRA horizontal winds (arrows) for July-August 2013 during the SEAC[4]RS time period. MLS observations of 100-hPa H_2O greater than 8 ppmv in this two-month period are shown by the white circles.

Figure 4. In each panel: left plot is water vapor retrievals from aircraft (color), aircraft with MLS averaging kernel (asterisks and lines) and MLS (black dots and lines) on 8 August 2013. Right plots are aircraft flight track and pressure profiles shown in color by longitude, and also MLS geolocations (asterisks and line). (a) Western CONUS MLS profiles and coincident aircraft profiles (blue), (b) Central CONUS Texas MLS profiles and coincident aircraft profiles (green), (c) Southern CONUS MLS profiles and coincident aircraft profiles (red).

Figure 5. Analysis of the 8 August 2013 NASA ER-2 aircraft flight. (a) Vertical profiles of JLH Mark2 *in situ* H_2O. Back trajectories were initialized from each of enhanced water measurements (blue). Initial water vapor mixing ratios for a subset of example trajectories are shown as red squares. (b) Example back trajectories (thin blue traces)

and coincident overshooting convection (red). Along the NASA ER-2 flight track (orange line), enhanced water vapor was measured (thick blue lines). This figure identifies where trajectories and OT are coincident (red) and nearly coincident within tolerances prescribed in Section 3.2 (green). The green symbols give an indication of the main regions of convective overshooting during the seven days prior to the ER-2 flight and which of those regions appeared to contribute most to the water vapor enhancement measured on the flight. (c) Altitude plot of example back trajectories showing coincident overshooting (red) and nearly coincident overshooting (green). The green symbols show the range of altitudes reached by the coincident overshooting convection and how many convective overshooting cells were nearby. The high resolution of the convective overshooting data meant that there could be multiple coincident convective overshooting cells for a single location on a back trajectory, (d) Days between OT and intercept by aircraft on 8 August 2013.

Figure 6. Analysis of the 16 August 2013 NASA ER-2 flight. (a) Vertical profiles of JLH Mark2 *in situ* H_2O similar to Figure 5a, (b) Back trajectories from the aircraft path similar to Figure 5b, (c) Altitude plot of back trajectories showing coincident overshooting (red) and nearly coincident overshooting (green) similar to Figure 5c, (d) Days between OT and intercept by aircraft similar to Figure 5d.

Figure 7. Analysis of the 27 August 2013 NASA ER-2 flight. (a) Vertical profiles of JLH Mark2 *in situ* H_2O similar to Figure 5a, (b) Back trajectories from the aircraft path similar to Figure 5b, (c) Altitude plot of back trajectories showing coincident overshooting (red) and nearly coincident overshooting (green) similar to Figure 5c, (d) Days between OT and intercept by aircraft similar to Figure 5d.

Atmos. Chem. Phys. Discuss., doi:10.5194/acp-2016-1065, 2016
Manuscript under review for journal Atmos. Chem. Phys.
Published: 19 December 2016

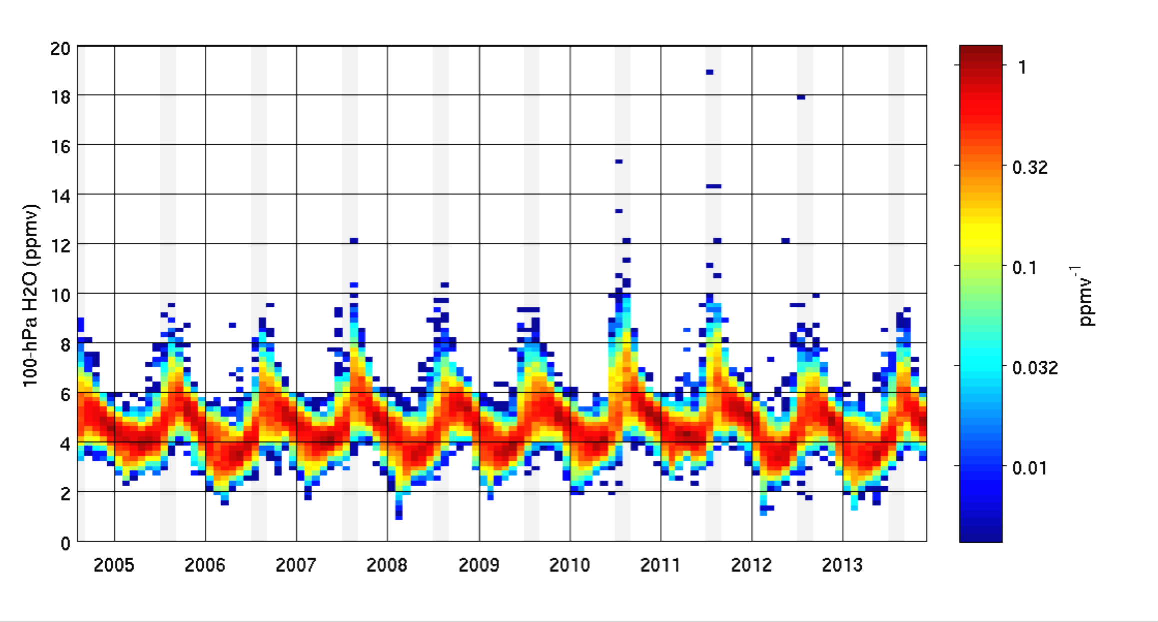

Figure 1. Time series of Aura MLS v3.3 100-hPa H_2O over North America. Each monthly histogram is normalized to unity over mixing ratio. Dashed black vertical lines mark year boundaries, and gray-shaded areas denote July-August. Data are from the eastern CONUS through northern Mexico (see Figure 2 insert), a study box empirically chosen to enclose the highest outliers associated with the North American Monsoon in the 10+ year MLS 100-hPa water vapor climatology (after Schwartz et al., 2013).

Atmos. Chem. Phys. Discuss., doi:10.5194/acp-2016-1065, 2016
Manuscript under review for journal Atmos. Chem. Phys.
Published: 19 December 2016

Atmospheric Chemistry and Physics
Open Access
Discussions

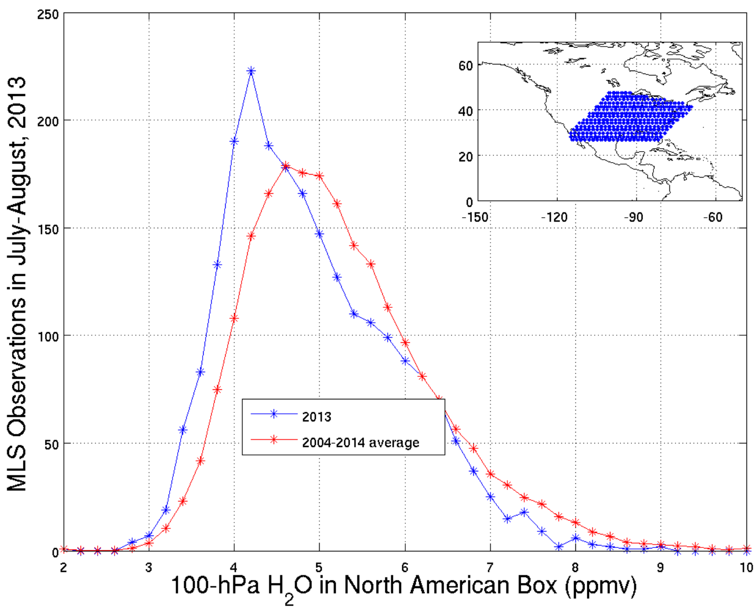

Figure 2. Distribution of Aura MLS July-August 100-hPa H_2O over North America (blue shaded box in insert) for July-August 2013 (blue line) and July-August ten-year mean for 2004 to 2013 (red line).

Atmos. Chem. Phys. Discuss., doi:10.5194/acp-2016-1065, 2016
Manuscript under review for journal Atmos. Chem. Phys.
Published: 19 December 2016

Atmospheric Chemistry and Physics
Open Access
Discussions

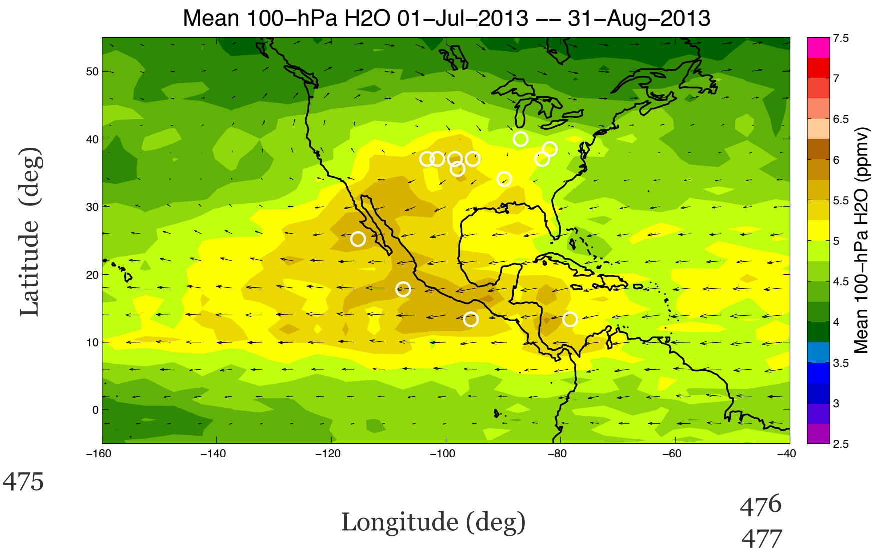

Figure 3. Aura MLS 100-hPa H_2O (color scale), with superimposed MERRA horizontal winds (arrows) for July-August 2013 during the SEAC[4]RS time period. MLS observations of 100-hPa H_2O greater than 8 ppmv in this two-month period are shown by the white circles.

Atmos. Chem. Phys. Discuss., doi:10.5194/acp-2016-1065, 2016
Manuscript under review for journal Atmos. Chem. Phys.
Published: 19 December 2016

Atmospheric Chemistry and Physics
Open Access
Discussions

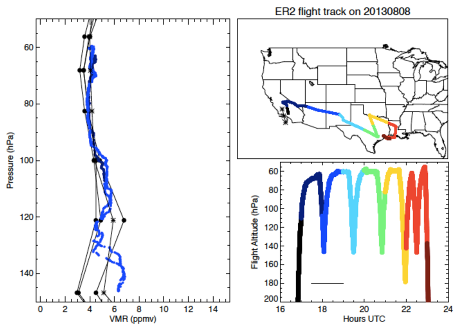

(a)

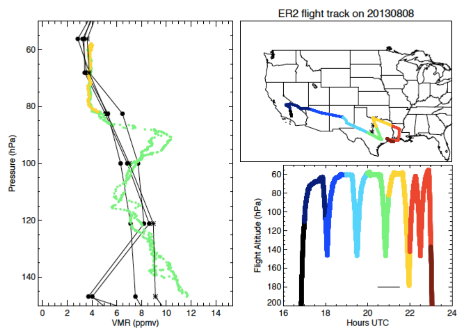

(b)

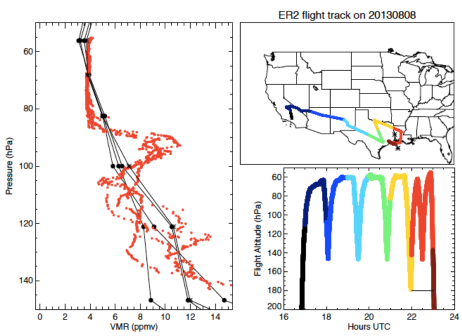

(c)

Figure 4. In each panel: left plot is water vapor retrievals from aircraft (color), aircraft with MLS averaging kernel (asterisks and lines) and MLS (black dots and lines) on 8 August 2013. Right plots are aircraft flight track and pressure profiles shown in color by longitude, and also MLS geolocations (asterisks and line). (a) Western CONUS MLS profiles and coincident aircraft profiles (blue), (b) Central CONUS Texas MLS profiles and coincident aircraft profiles (green), (c) Southern CONUS MLS profiles and coincident aircraft profiles (red).

Atmos. Chem. Phys. Discuss., doi:10.5194/acp-2016-1065, 2016
Manuscript under review for journal Atmos. Chem. Phys.
Published: 19 December 2016

Atmospheric Chemistry and Physics
Open Access
Discussions

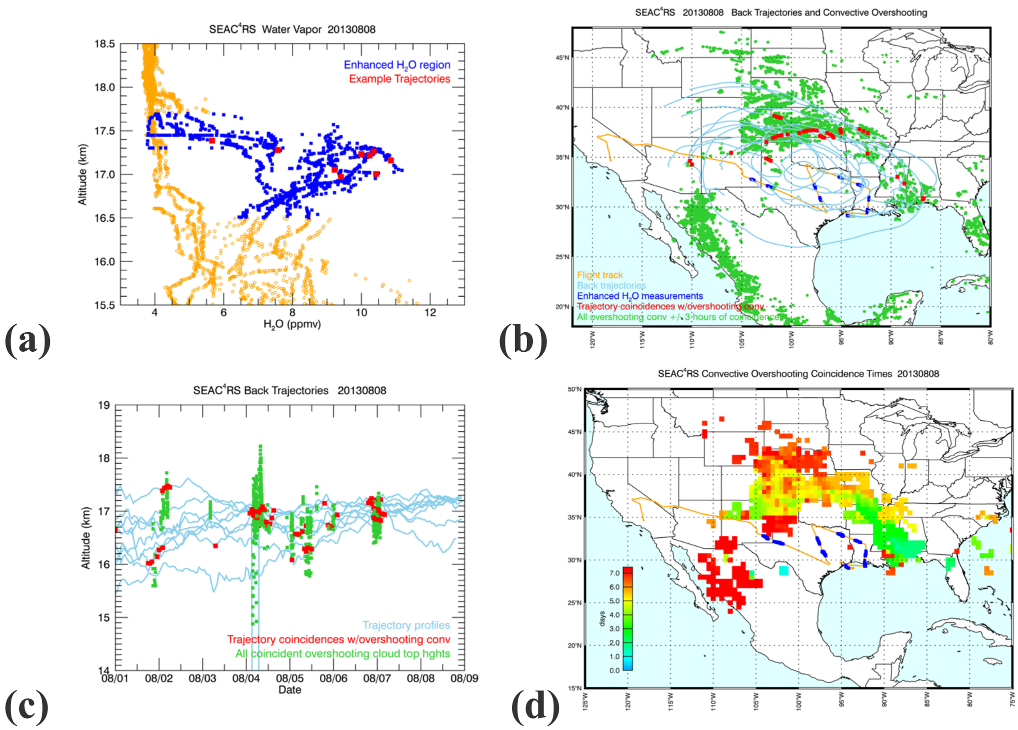

Figure 5. Analysis of the 8 August 2013 NASA ER-2 aircraft flight. (a) Vertical profiles of JLH Mark2 *in situ* H_2O. Back trajectories were initialized from each of enhanced water measurements (blue). Initial water vapor mixing ratios for a subset of example trajectories are shown as red squares. (b) Example back trajectories (thin blue traces) and coincident overshooting convection (red). Along the NASA ER-2 flight track (orange line), enhanced water vapor was measured (thick blue lines). This figure identifies where trajectories and OT are coincident (red) and nearly coincident within tolerances prescribed in Section 3.2 (green). The green symbols give an indication of the main regions of convective overshooting during the seven days prior to the ER-2 flight and which of those regions appeared to contribute most to the water vapor enhancement measured on the flight. (c) Altitude plot of example back trajectories showing coincident overshooting (red) and nearly coincident overshooting (green). The green symbols show the range of altitudes reached by the coincident overshooting convection and how many convective overshooting cells were nearby. The high resolution of the convective overshooting data meant that there could be multiple coincident convective overshooting cells for a single location on a back trajectory, (d) Days between OT and intercept by aircraft on 8 August 2013.

Atmos. Chem. Phys. Discuss., doi:10.5194/acp-2016-1065, 2016
Manuscript under review for journal Atmos. Chem. Phys.
Published: 19 December 2016

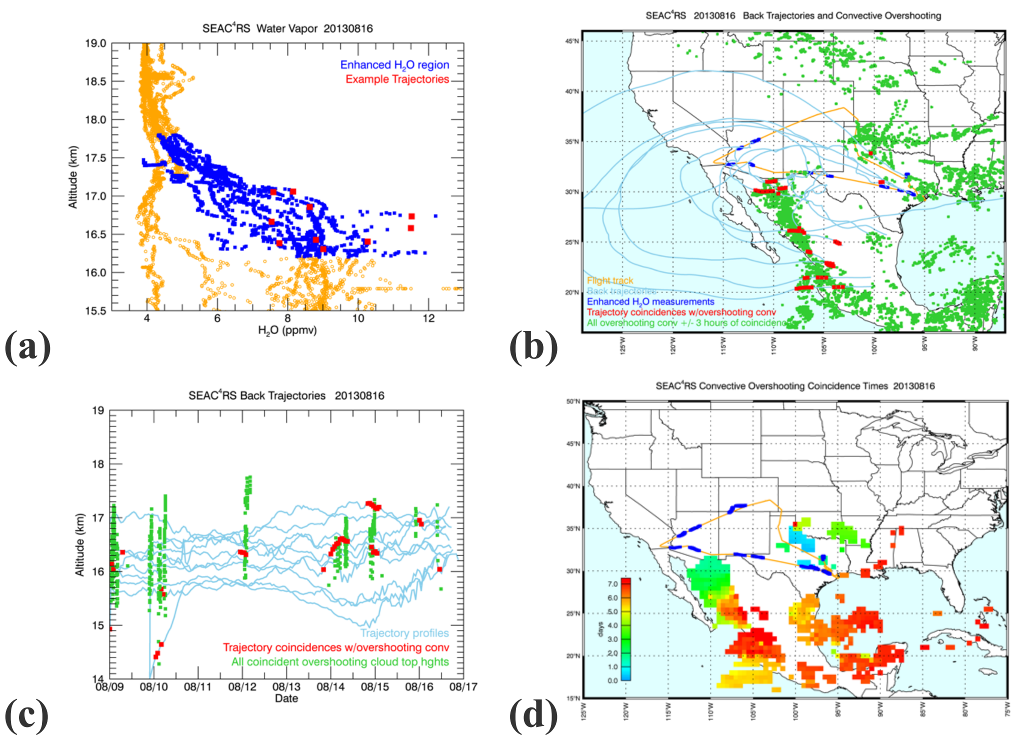

Figure 6. Analysis of the 16 August 2013 NASA ER-2 flight. (a) Vertical profiles of JLH Mark2 *in situ* H_2O similar to Figure 5a, (b) Back trajectories from the aircraft path similar to Figure 5b, (c) Altitude plot of back trajectories showing coincident overshooting (red) and nearly coincident overshooting (green) similar to Figure 5c, (d) Days between OT and intercept by aircraft similar to Figure 5d.

Atmos. Chem. Phys. Discuss., doi:10.5194/acp-2016-1065, 2016
Manuscript under review for journal Atmos. Chem. Phys.
Published: 19 December 2016

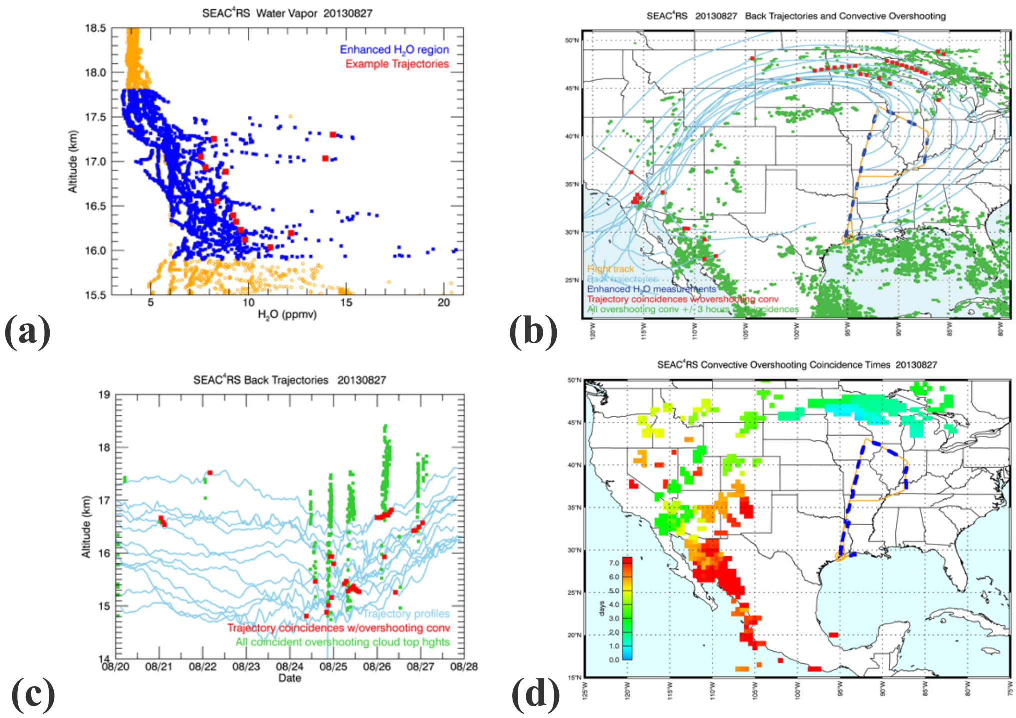

Figure 7. Analysis of the 27 August 2013 NASA ER-2 flight. (a) Vertical profiles of JLH Mark2 *in situ* H_2O similar to Figure 5a, (b) Back trajectories from the aircraft path similar to Figure 5b, (c) Altitude plot of back trajectories showing coincident overshooting (red) and nearly coincident overshooting (green) similar to Figure 5c, (d) Days between OT and intercept by aircraft similar to Figure 5d.